PCCP

ROYAL SOCIETY OF CHEMISTRY

COMMUNICATION

View Article Online
View Journal | View Issue

Cite this: *Phys. Chem. Chem. Phys.*, 2026, **28**, 14373

Received 26th March 2026,
Accepted 1st June 2026

DOI: 10.1039/d6cp01096b

rsc.li/pccp

HyDRA-II: spectroscopic results and BEsT guesses for the mono- and dihydrate blind challenge

Margarethe Bödecker, Eaindra Lwin, Finn Knüppe, Noah O. Evers, Elisabeth Sennert, Moritz Niessner, Nils O. B. Lüttschwager and Martin A. Suhm *

HyDRA blind challenges aim at unbiased forecasts of water vibrations in vacuum-isolated hydrate complexes of organic molecules by different computational protocols. In this work, directly after the completion of the HyDRA II challenge and ignorant of its computational results, the experimental findings for the 9 new solvates with a total of 12 hydrogen-bonded water OH stretching wavenumbers are disclosed and discussed. We further summarise and analyse the 70 entries of the training database, which were made available at the start of the challenge. Monohydrates of 4 other previously uncharacterised solvates are added to support the assignment of the blind test entries and to widen the future training database. The compounds for which gas phase monohydrate OH stretching fundamentals are reported for the first time comprise a difluorobenzonitrile, a difluorobenzoic acid, eucalyptol, an iodo-methyl-pyrazole, a methoxypyridine, Hünig's base, a pyrrolidine ethanol, TEMPONE, diethylhydroxylamine, pyrazine, pyrimidine, a triazine and a chiral chloropropionic acid. An experimental bridging approach (Bridging Experiments by Theory, or in short BEsT guess) using inexpensive harmonic density functional theory predictions from the training database for educated guesses of unknown vibrational wavenumbers is proposed to assist the future evaluation of the blind challenge. Proposals on how to compare computational predictions to experiment depending on the employed level of anharmonic perturbation are made. It will be interesting to see how different computational protocols perform in the wide range between outstanding predictions (root-mean-square deviation <10 cm^{-1}) and placebo-quality deviations (>100 cm^{-1}) for the 12 disclosed wavenumbers.

Quantum-chemical methods are very useful and versatile tools for experimental spectroscopists. The spectroscopists choose their favourite approximations for daily work, often based on anecdotal evidence and previous experience. Unfortunately, almost any plausible but incorrect individual experimental result can be confirmed by some variant of some computational model (see SI chapter 1 for an example). Therefore, it is helpful to initially hide selected, secured experimental results, while challenging different computational chemistry groups to make unbiased predictions based on their favoured models.[1–4] These predictions should also be hidden from the experimentalists in order not to bias the spectral assignments.[4] The resulting double-blind challenge profits from a well-curated training set of related experimental data, but computational participants are free to use or ignore this offer when making their predictions for the undisclosed test set.

While electronic spectroscopy exhibits the stronger quantisation, it has been recognised from the start of modern quantum mechanics that suitable approximations for the quantum nature of nuclear motion beyond the harmonic oscillator approximation are essential as well,[5] when comparing to experimental observables. This is clearly the case when hydrogen nuclei are involved. Usually, the true bottleneck for reliable predictions is not the Born–Oppenheimer or Born–Huang approximation for the separation of electronic and nuclear motion.[6] Instead, it is the combination of approximations within the electronic and nuclear parts, which may sometimes create the illusion of an excellent performance (see SI chapter 1 for an example) when more or less systematic cancellation between or within electronic and nuclear approximation errors is actually in place.[7,8] Systematic error cancellation can be very useful for the practical spectroscopist, but it is easily lost when extrapolating too far from the training base. Therefore, the training database for spectroscopic observables needs to be periodically extended, to reduce extrapolation in favour of interpolation and to identify the most powerful quantum-chemical approximations available.

A field of hydrogen-probing vibrational spectroscopy with particular relevance for the persistent challenge of explicit solvation modelling[9] is microhydration of organic molecules in the gas phase.[10–12] HyDRA (**Hy**drate **D**onor **R**edshift **A**nticipation) is a series of double-blind challenges and database extensions in this field.[13,14] Cold, isolated mono- and dihydrates of organic molecules are generated in supersonic jet expansions and their intense, hydrogen bond-sensitive water

Institut für Physikalische Chemie, Universität Göttingen, Tammannstr. 6, 37077 Göttingen, Germany. E-mail: msuhm@uni-goettingen.de

OH stretching (OHb) transitions are recorded by infrared or Raman spectroscopy.[15–17] To predict the transition wavenumbers (and equivalently the down- or redshift relative to the symmetric stretching fundamental of isolated water molecules,[4] experimentally observed at 3657 cm^{-1}), one may combine any electronic structure treatment of the complex with an appropriate model of the vibrational dynamics or one may use some kind of empirical training and interpolation protocol.[12]

Hydrogen-bonded water OH stretching states in microhydrate complexes are often nicely isolated from other fundamental vibrations, but sometimes they come close to one[18] or more[19] combination states which involve several quanta in other motions of the water molecule, as sketched in Fig. 1. These local perturber (lp) states typically carry negligible infrared and Raman intensity on their own (lp^0), but if they share the same symmetry and some coupling with the water OHb stretch due to the large amplitude motion of the solvating water unit, they can borrow intensity and stretching character by wavefunction mixing, thus reducing the purity or intensity of the bright transition to a fraction $P < 1$ of its intrinsic intensity in the raw spectrum (see Fig. 1). The deperturbed location of the OHb transition (OHb^0) is then close to the intensity centroid of the coupled modes involved in the intensity sharing.[18] Any computational model which averages over such local couplings is therefore advised to compare its predictions to the OHb^0 centroid or deperturbed (dep) band position (central trace in Fig. 1), whereas fully anharmonic coupling models can directly address the dominant OHb transition and its purity P in the raw spectrum (upper trace in Fig. 1).

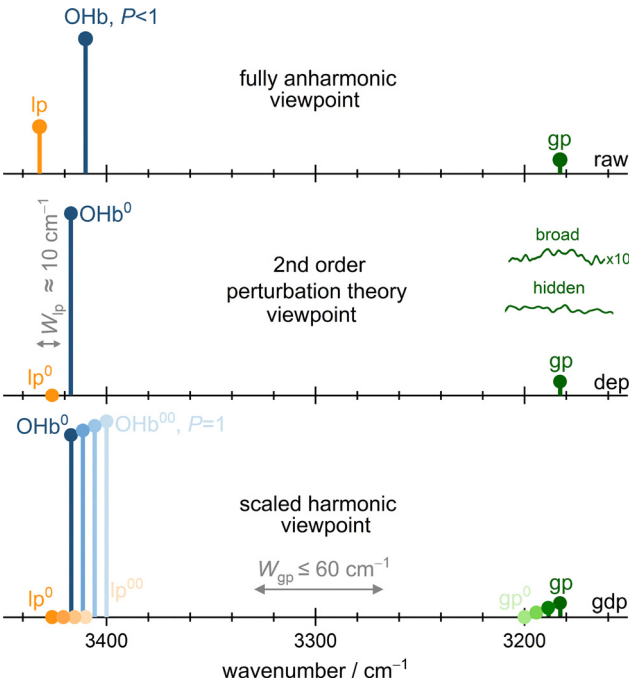

Fig. 1 Different interpretations of a raw experimental stick spectrum (upper trace) with an OHb stretching transition, a local perturber (lp) stealing some OHb character and the distant water bending overtone which may act as a global perturber (gp) by also stealing some intensity from OHb, leaving only a fractional intensity $P < 1$ in the main transition. Computational methods which miss out local perturbations are expected to perform better when compared to the deperturbed middle trace (dep), where the effect of lp in the experimental spectrum is removed by transferring its intensity to OHb and by correcting the OHb position for the resonance shift (OHb^0). If the long-distance Fermi resonance of OHb^0 with the water bending overtone as a global perturber (gp) is also neglected by the model (such as in scaled harmonic approaches), a globally deperturbed OHb^{00} position (gdp) may offer the best comparison (lowest trace). However, at long distance, with unknown magnitude of the normal mode Fermi coupling matrix element (likely $\lesssim$60 cm^{-1}) and unknown intrinsic intensity of the hardly visible gp state, this often can only be estimated as a worst case asymmetric uncertainty, illustrated by the comb of conceivable OHb^{00} states drawn with fading color in the lower trace.

By far the strongest and longest-range coupling expected for OHb is a Fermi resonance with the 2-quantum water bending overtone[17] b2 of the same water molecule (generalised to gp for global perturber in Fig. 1). Basically, its influence is always there, even if it may not be as apparent in the experimental spectrum as a local resonance due to the large spectral separation and the weak intensity transfer. This low-order coupling between OHb and b2 is usually captured to some extent by second order vibrational perturbation theory approaches and their variants.[20] Therefore, such leading order perturbation approaches as well as restricted variational treatments of this Fermi resonance are advised to compare their results to the locally deperturbed (dep) experimental values as well, unless they also include an explicit treatment of any local perturbers.

This is not the case for the popular scaled harmonic calculations, where the harmonic prediction ω is multiplied by some scaling factor σ due to a mix of electronic structure deficiencies and neglected anharmonic contributions, to better match experiment. Such a scaled harmonic approach is blind to any resonances, be they local (lp) or more global (gp). Therefore, uniformly scaled harmonic approaches are expected to deviate systematically whenever OHb and b2 approach each other due to strong hydrogen bonding and the resulting Fermi resonance shifts become pronounced. In this range of hydrogen bond strengths, scaled harmonic approaches trained on weaker hydrogen bonds are thus expected to be somewhat off for the right reason, when compared to either raw or locally deperturbed (dep) reference values. If OHb is observed with a wavenumber above b2, they are likely to underestimate this perturbed OHb wavenumber. If it is below b2, they are expected to overestimate the actual OHb wavenumber. By assuming an upper limit of the Fermi resonance coupling strength ($W \approx 60$ cm^{-1}, as for concerted bending overtones in cyclic water clusters[17]), we encode the worst case effect of this global perturbation into one side of the experimental uncertainty estimate, even if the b2 perturber remains hidden in the noise, perhaps due to excessive lifetime broadening (see Fig. 1), perhaps due to interference with intrinsic bending overtone intensity. This asymmetric extended uncertainty is thus a service to scaled harmonic approaches in the range of strong hydrogen bonding. Because the asymmetric uncertainty only applies to cases where the gp (b2) is too weak or broad to be explicitly included into an experimental deperturbation, one can drop it in the case of amine monohydrates, where

the hydrogen bonds are of the right strength to redistribute significant intensity from OHb to both lp and gp (b2) states.

Are scaled harmonic approaches useful at all in the field of hydrogen bonding? For weaker hydrogen bonds, they have been quite successful by exploiting the partial cancellation of anharmonic effects, as demonstrated in the first HyDRA blind challenge.[13] By looking at the shift between water monomer and complexed water instead of absolute wavenumber predictions and by adding this shift to the experimental monomer value, they circumvent the need for explicit anharmonicity along the OH bond, but they are blind to the strong b2 Fermi resonance and are thus expected to perform poorly for OHb in the neighbourhood of b2. Our proposed global deperturbation analysis (gdp) alerts to this by quoting extended uncertainties. It cannot fix the perturbation and therefore does not change the central complex OHb^0 wavenumbers from the local deperturbation approach (dep), because the Fermi coupling constant remains experimentally undetermined at a distance. If, however, the Fermi resonance between OHb and b2 is already part of the local resonance analysis within the dark state approximation, such as in tertiary amine monohydrates,[19] there is no need to increase the one-sided uncertainty estimate and the (dep) and (gdp) approaches are essentially identical, apart from a subtle effect on the monomer reference, which slightly feels the effect of the distant b2 state through a reduced Fermi resonance coupling constant (see SI section 2.5).

In the first HyDRA challenge, the scope was relatively narrow (10 monohydrates in the test set with only weak to medium strength hydrogen bonds) and several different strategies were quite successful. With the current HyDRA II extension to stronger hydrogen bonds and cooperative double hydration, it should become evident which approaches remain successful, which ones can be improved and which novel approaches might emerge. For this purpose, the training database was substantially extended from 10 to 70 curated experimental OHb stretching wavenumbers and from a wavenumber spread of about 200 cm^{-1} to more than 600 cm^{-1}. The new test set consists of 7 monohydrate and 3 dihydrate wavenumbers. It is complemented by a bonus set of 2 monohydrates, for which the experimental assignment was particularly challenging due to either open-shell character and overlapping resonances or a missing training counterpart.

The core test set includes five nitrogen acceptors with widely different hydrogen bond acceptor strength: an aromatic nitrile (DFB), an NH-protected and iodinated pyrazole (IMP), a methoxypyridine (MOP), the bulky tertiary amine known as Hünig's base (DPA) and an amino alcohol[21] (PYE). In addition to monohydrates, dihydrates are characterised for Hünig's base (only the indirectly bound water, because the directly bound water overlaps with the CH stretching region) and for the pyrazole derivative (both water molecules). The pyrazole derivative is relatively far from any training set members, in particular when it binds two water molecules. Two oxygen acceptors, a benzoic acid derivative (FBA) and a bulky ether (EUC), are more similar in their bond strength towards a single water molecule, but differ in the number of hydrogen bonds and thus cooperativity. The two bonus monohydrates involve a bifunctional nitroxyl radical[22] with closely competing binding sites (OTM) and a hydroxylamine (DHA), for which no chemically similar training set member is available. The monohydrate of OTM shows evidence for a local resonance, perhaps in both conformations. DPA has conformational isomerism which may depend on hydration but is not critical for the position of the OHb fundamental, which shares intensity with 2–3 perturber states like other tertiary amines. For FBA, a weak local resonance cannot be ruled out but this possibility is absorbed in the uncertainty of the quoted band position. Table 1 and Fig. 2 present the experimental results for the test and bonus sets in a compact form.

For our experimental and assignment strategies, we largely refer to the SI (chapters 2, 4–6). Table 1 offers three sets of reference values of OH stretching fundamental wavenumbers (raw, dep, gdp) which different theory levels may want to address, as discussed above. The (pre-)publication of this table in the present work ends the HyDRA II blind challenge period for theory participants and it forms the basis of later joint and individual evaluations of the performance of the proposed computational models.

Table 1 Raw and deperturbed (dep) experimental wavenumbers $\tilde{\nu}_{exp}$ in cm^{-1} of the monohydrate (1) and some dihydrate (2i: indirect contact with the acceptor; 2d: direct contact) OHb fundamentals of the test and bonus set acceptors ACC. $P_{min,max}$ span the experimental intensity fraction of the total OHb intensity attributed to the strongest signal (see SI section 2.4). Experimental wavenumber uncertainties in parentheses are given as super-/subscripts when unsymmetric. They are extended unsymmetrically (gdp column) for comparison to computations which systematically neglect the strong bending overtone resonance. The respective wavenumber shifts are listed in Tables S9 and S20

ACC-OHb	$\tilde{\nu}_{exp}$ (raw)	P_{max} P_{min}	$\tilde{\nu}_{exp}$ (dep)	$\tilde{\nu}_{exp}$ (gdp)
DFB-1	3614(1)	1.00 0.90	3614(1)	3614^{+03}_{-08}
FBA-1	3530(2)	1.00 0.80	3530(10)	3530^{+12}_{-19}
EUC-1	3509(1)	1.00 0.90	3509(1)	3509^{+03}_{-11}
IMP-1	3482(1)	1.00 0.90	3482(1)	3482^{+03}_{-12}
IMP-2d	3367(4)	1.00 0.90	3367(4)	3367^{+06}_{-26}
IMP-2i	3492(2)	1.00 0.90	3492(2)	3492^{+04}_{-12}
MOP-1	3458(1)	1.00 0.90	3458(1)	3458^{+03}_{-13}
DPA-1	3273(2)	0.60 0.45	3266(6)	3266^{+08}_{-05}
DPA-2i	3489(2)	1.00 0.90	3489(2)	3489^{+04}_{-13}
PYE-1	3101(6)	1.00 0.90	3101(6)	3101^{+30}_{-05}
OTM-1	3494(1)	0.80 0.55	3500^{+03}_{-07}	3500^{+05}_{-17}
DHA-1	3362(5)	1.00 0.90	3362^{+09}_{-05}	3362^{+11}_{-28}

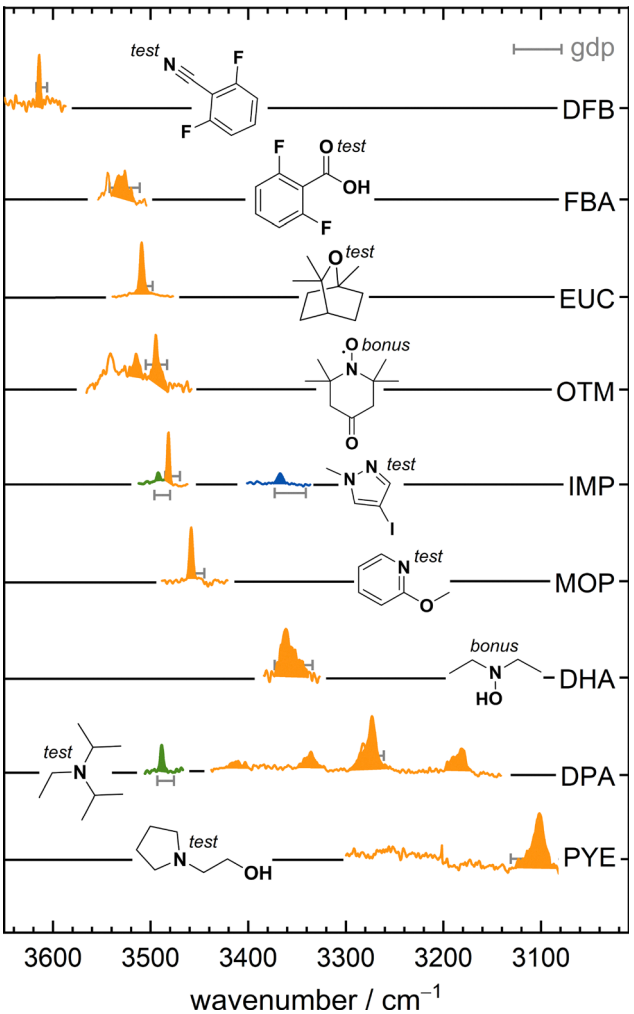

Fig. 2 Lineup of spectral segments for the 9 test and bonus mono- (orange) and dihydrates (green for indirect and blue for direct hydration), showing the increase in anharmonic couplings and spectral broadening with increasing hydrogen bond strength from top to bottom, also resulting in larger uncertainties for global deperturbation (gdp, grey horizontal bars) of the OH stretching motion.

Table 2 Raw and deperturbed (dep) experimental wavenumbers $\tilde{\nu}_{exp}$ in cm^{-1} of the monohydrate OHb fundamentals of 1,3,5-triazine (TRZ), (*S*)-(−)-2-chloropropionic acid (CPA), pyrazine (PRZ) and pyrimidine (PYM). $P_{min,max}$ span the experimental intensity fraction of the total OHb intensity attributed to the strongest signal (see SI section 2.4). Experimental wavenumber uncertainties in parentheses are given as super-/subscripts when unsymmetric. They are extended unsymmetrically (gdp column) for comparison to computations which systematically neglect the strong bending overtone resonance

ACC-OHb	$\tilde{\nu}_{exp}$ (raw)	$\frac{P_{max}}{P_{min}}$	$\tilde{\nu}_{exp}$ (dep)	$\tilde{\nu}_{exp}$ (gdp)
TRZ-1	3553(1)	1.00 0.90	3553(2)	3553^{+04}_{-10}
CPA-1	3529(3)	1.00 0.80	3529(9)	3529^{+11}_{-18}
PRZ-1	3519(1)	0.65 0.50	3511(2)	3511^{+04}_{-12}
PYM-1	3499(1)	1.00 0.80	3503(4)	3503^{+06}_{-14}

To further extend the HyDRA database beyond the existing 70 wavenumbers and the 12 new wavenumbers of HyDRA II, we also present the spectra for 4 closely related systems (Table 2). These extra systems were studied to secure some HyDRA II assignments, based on their chemical similarity and expected analogies in the spectra. For that purpose, they can be bundled with related test and training systems and their experimental trends are compared to harmonic B3LYP calculations. Parallel trends across the systems between harmonic calculation and raw as well as dep(erturbed) experimental values help to confirm smaller deperturbations due to local resonances. Details are provided in chapter 6 of the SI. As an example, Fig. 3 shows the effects of what we call a b2lib deperturbation[18] on five monohydrates for related N-heterocycles. Their OHb transitions fall in a narrow range of less than 100 cm^{-1}, where the combination band between the water bending overtone (b2) and a librational (lib) motion of the hydrogen-bonded water against the acceptor (b2lib) is also predicted. If the level coincidence is comparable to the anharmonic coupling constant (about 10 cm^{-1}), the lp scenario described in Fig. 1 comes into play. No resonance with this potential perturber state is observed for the training member pyridine, the test set member 2-methoxypyridine, or 1,3,5-triazine as an extra system. In each case, a single OHb band is correspondingly found. However, the two extra systems pyrazine[23] and pyrimidine show characteristic spectral splittings, likely due to the resonating b2lib state. In the case of pyrimidine,[24] the evidence is less clear and only compatible with a very broad (short-lived) local perturber, almost hidden within the noise (SI, chapter 6). It is rewarding to see that the experimental trends after deperturbation (orange) are even better aligned with the scaled harmonic predictions than the trends for the dominant raw transitions (grey). It is further rewarding to observe this resonance, which had previously been observed mainly for ketone,[18] nitroxyl,[22] and tentatively also carboxylic acid[25] monohydrates, at a similar wavenumber and with a similar coupling strength for the chemically different N-heterocycles. To further underscore the resonance interpretation, we compare to a Raman spectrum (SI, chapter 6), which must look basically the same, if the intensity pattern results from wavefunction mixing instead of electrical transition moments. As expected, this kind of bend-librational resonance in hydrogen-bonded water is thus quite universal, whenever the water OHb stretching vibration comes close to 3500 cm^{-1} and a librational mode has the right force constant for bridging the gap to the bending overtone b2 of the same water molecule. It is remarkable that a higher order anharmonic resonance in a solvating water molecule with a coupling constant on the order of 10 cm^{-1} is so robust across the chemical space, given the wide variation in hydrogen bond anisotropy for nitroxyl-, carbonyl- and N-heterocyclic acceptors. Perhaps, the HyDRA II challenge will motivate theoretical spectroscopists to rigorously analyse this regularity beyond our simplistic effective coupling models. In the first HyDRA challenge, none of the theoretical approaches did address this

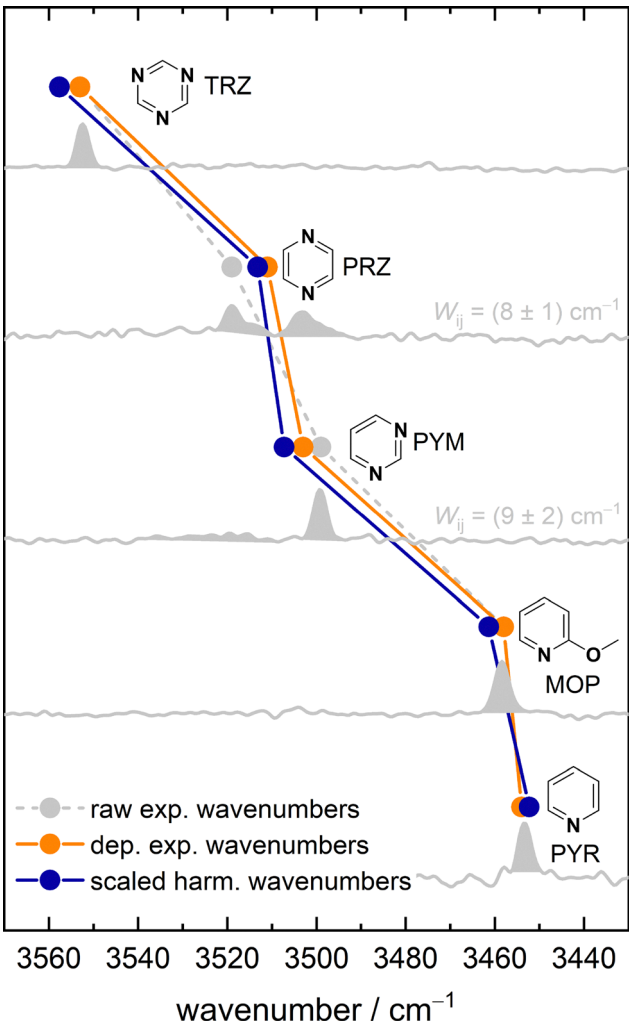

Fig. 3 Trends in N-heterocycle monohydrate OHb wavenumbers from the HyDRA database[14] (PYR) and from this work (TRZ, PRZ, PYM, MOP). Scaled harmonic wavenumbers (B3LYP-D3(BJ,abc)/def2-TZVP, σ = 0.98) are shown in blue, raw experimental wavenumbers are shown in grey and deperturbed experimental wavenumbers are shown in orange. For each system, the jet-spectrum is shown in grey and the assigned bands are filled. After deperturbation (coupling matrix elements W_{ij} in grey), the experimental wavenumber trend is even better reproduced by theory than before.

higher order resonance explicitly, although it was part of the training set and cannot be ruled out in some test set members.

While we are looking forward to the most powerful computational models which are able to truly predict the HyDRA II experimental results, it makes sense to contemplate on alternative predictive methods for OHb stretching wavenumbers which are available to experimentalists who only have routine computational models at their disposal, typically based on density functional theory (DFT). The idea is to use some inexpensive but reasonably complete density functional, likely including London dispersion correction, to make harmonic predictions of the OHb stretching fundamental in the relevant complexes, and to transfer the required harmonic scaling factor(s) σ to match experiment, from one or more known training complexes to an unassigned test complex. The hope is that sufficiently similar training systems will have similar electronic structure and anharmonic errors, which may partially cancel in the difference and lead to robust forecasts. We call this family of interpolations BEsT guesses (schematically depicted in Fig. 4), where BEsT stands for **B**ridging **E**xperiment**s** by **T**heory. Note that they are not blind in the present case (although efforts were made to ignore the experimental test system wavenumbers when deciding for an interpolation sampling) and thus should not be compared in their performance to the future results of the HyDRA II blind challenge. BEsT guesses may include pitfalls such as incorrect predictions of the relevant global minimum structure of the complex by the inexpensive density functional or a lack of sufficiently similar compounds in the training database, but they are straightforward to obtain. BEsT guesses are experimentalist's substitutes as long as theory is not powerful enough to provide unbiased accurate predictions on a regular basis.

We explore two different BEsT guess distance metrics in the present work, using the standard harmonic B3LYP-D3(BJ,abc)/def2-TZVP model as a bridging tool. A qualitative metric is chemical similarity and a quantitative metric is harmonic wavenumber proximity, both referring to the database of 70 training wavenumbers. The starting point is to use all 70

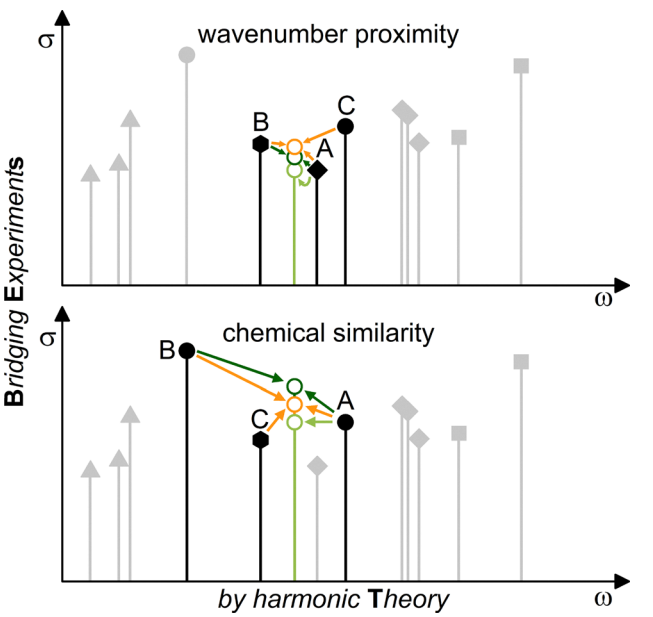

Fig. 4 Schematic sketch of the BEsT guess approach: Among the various individual scaling factors σ which bring simple harmonic DFT OHb predictions ω into agreement with experiment for a large number of training systems (vertical grey bars, ending in filled symbols which stand for different functional groups), the 1, 2 or 3 closest (black bars, A, B, C) in harmonic wavenumber ω (top part) or chemical structure (bottom part, filled circle ≈ filled hexagon, symbolizing similar but not identical functional groups such as a formyl and a keto group) to a test candidate (coloured bar) are used to guess its experimental wavenumber in the form of the best scaling factor to be applied to its harmonic DFT prediction (unfilled circles, adopting the scaling factor from A (light green), from the average of A and B (dark green), or from the average of A, B, C (orange)).

experimental wavenumbers to obtain the average scaling factor ($\bar{\sigma}_{70} = 0.9768$) for the best overall match as well as the RMSD (root-mean-square deviation) between the uniformly scaled computed harmonic values and their experimental counterparts. This training-RMSD is a measure for the average prediction quality of the chosen scaled harmonic approach. The average scaling factor can now be applied to harmonic predictions for the full set or a partial set of blind test candidates and provides a test-RMSD in comparison to the test set experiment. This test-RMSD should be relatively close to the training-RMSD, if the training and test sets are sufficiently similar. In our case, the training- (based on 70 samples) and test-RMSD (based on 12 samples) values amount to 23.5 cm^{-1} and 26.1 cm^{-1}, respectively. They are not as poor as one might have expected, given that they correspond to the performance of a single-parameter linear fit of the harmonic model to the experimental training data only.

To further improve the test-RMSD, one can now remove training set members from the procedure which are distant from the test set in terms of either chemical similarity or computed wavenumber proximity. This can be done on an individual basis for each test system, leaving only the 1–3 most related training members (A, B, C), either based on chemical similarity or based on harmonic wavenumber proximity. This small individual set of most similar training systems for a given test system is used to determine an optimised scaling factor which is then transferred to the test system. Instead of using individual matches for each test system, one can also consider the average scaling factor for the collective set of individual matches to predict all 12 hydrate wavenumbers at the same time. Depending on the diversity of the test set, this will typically result in a poorer RMSD than individual matches. This formalised procedure mimics the intuitive prediction strategy of an experimentalist, who uses a moderate quality theory model to relay pre-existing spectroscopic information from known to new systems.

Fig. 5 gives examples of such BEsT guess RMSD values for different test sets (for a more detailed analysis see chapter 7 in the SI). If one considers all 12 entries of the present blind test, there is no substantial advantage in restricting the BEsT guesses to the chemically or spectrally individually closest three training members, rather than using the merged set of training systems. The training set is apparently not close enough to the test set, such that individual outliers dominate the test-RMSD. This is confirmed by analysing the consequence of leaving away the three largest outliers in the test set. Now, there is a significant improvement in particular when the BEsT guess is performed on the individually closest three training members, down to a test-RMSD of 6 cm^{-1}. If one alternatively restricts the BEsT guess to the 6 monohydrates with a single OHb fundamental and leaves out the cooperative systems, the predictions also get better. Chemical similarity and even more so wavenumber proximity again reduce the RMSD significantly, if one restricts the interpolation to the 3 most similar training members, down to a test-RMSD of 6 cm^{-1}. When interpolating all 6 non-cooperative monohydrates with the same scaling factor

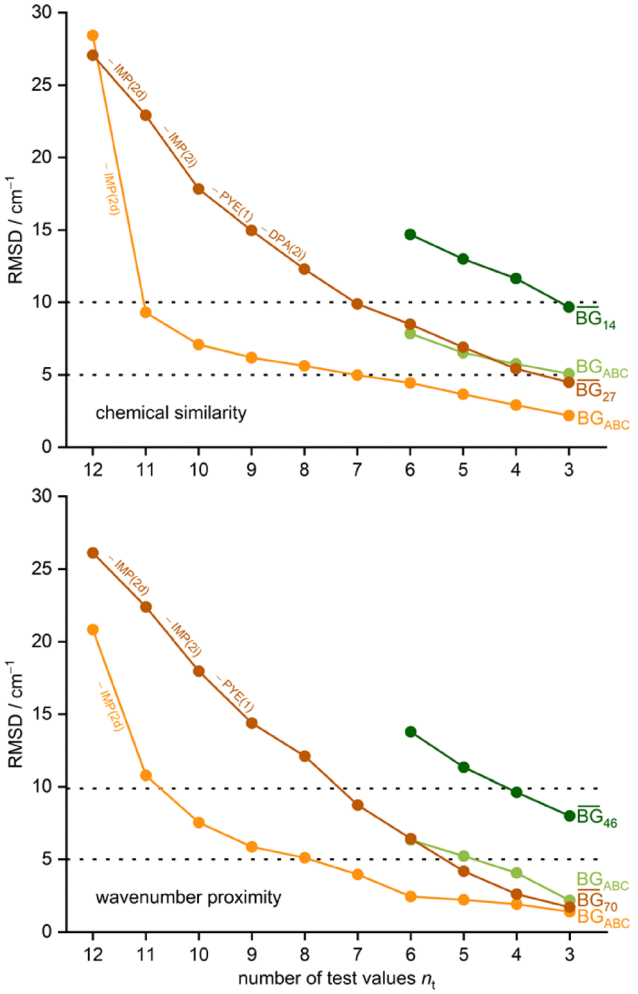

Fig. 5 Progressively improving test-RMSD values by successively removing the largest test set outliers based on the complete training set ($\overline{BG}_{70}$, $\overline{BG}_{27}$, brown) or the individually best-fitting 3 training members (BG_{ABC}, orange) for the entire test and bonus set (12 wavenumbers) or the 6 non-cooperative monohydrates only ($\overline{BG}_n$, dark green and BG_{ABC}, light green), based on chemical similarity (upper part, including $\overline{BG}_{14}$) or wavenumber proximity (lower part, including $\overline{BG}_{46}$). The largest outliers (indicated next to the connecting lines) include several cooperative systems containing two OHb groups (3 dihydrate wavenumbers and 1 alcohol monohydrate wavenumber). For the 6 systems, RMSD values for BEsT guesses based on the training set around and below 10 cm^{-1} are feasible even for a harmonic DFT model (see Table S35).

(obtained from the merged training subset), the RMSD values are significantly larger, but still much better than for the full set of 12 mono- and dihydrate wavenumbers. Harmonic DFT OHb wavenumbers apparently cannot describe in a satisfactory way mono- and dihydrates, systems with OHb wavenumbers higher and lower than b2 or strong and weak hydrogen bonds at the same time.

The present work discloses and describes the experimental results which were largely collected in 2025 for the HyDRA II blind challenge, about one Olympiad after HyDRA I,[4] together with an analysis and exploitation of the training database[14] published in mid-2025. The raw spectral wavenumbers

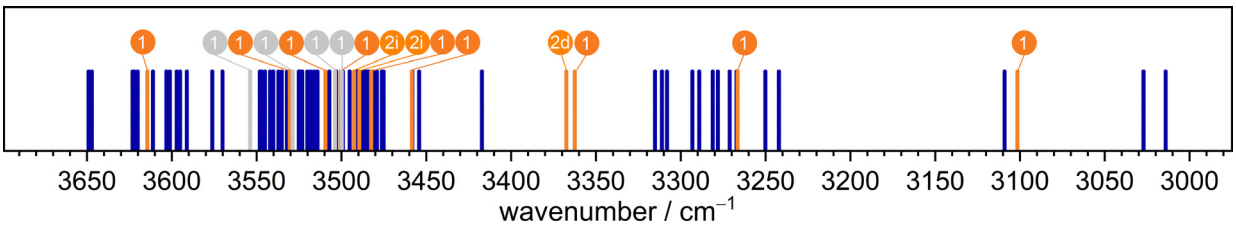

Fig. 6 OHb wavenumber distribution (dep) of the current HyDRA database[14] (blue) together with the 16 new entries from this work. HyDRA II test (10) and bonus (2) set wavenumbers are shown in orange, 4 further additions are shown in grey. This figure illustrates that the HyDRA II test and bonus sets cover a broad wavenumber range (513 cm^{-1}) which is still enclosed by the range of the full training set.

reported in this work represent our best possible reference for accurate theoretical models, but we make efforts to invite more approximate models by deperturbing for anharmonic resonances. Fig. 6 shows that the presented (deperturbed) core test (10), bonus test (2) and extra (4) wavenumbers are enclosed by the training base (70), together spanning about 80% of the previously outlined training range. Of particular interest will be the computational model performance for cooperative dihydrates, for swapped OHb-b2 wavenumber sequences and for the hydroxylamine case (with no functional group training available). Our BEsT guess analysis indicates that there is potential for models with RMSD values around 10 cm^{-1} or even below, at least for monohydrates of acceptors without their own OH group which could lead to harmonic mode mixing. Such a $< 2\%$ prediction performance relative to the span of red shifts would indeed be impressive for the combined challenge of getting the electronic structure right and capturing the various anharmonic effects. It would allow for a new era of vibrational spectroscopy in the field of microsolvation, where theory can start to replace selected spectroscopic experiments rather than to only assist their assignment and interpretation. On the other hand, the average of the 12 blind test wavenumbers of HyDRA II is 3431 cm^{-1} (compared to 3469 cm^{-1} for the 70 available training wavenumbers) and their RMSD from this average is 132 cm^{-1} (compared to 135 cm^{-1} for the 70 available training wavenumbers). Therefore, computational models which have an RMSD larger than about 100 cm^{-1} in comparison to the 12 experimental test set wavenumbers do not perform significantly better than an optimised null hypothesis (or kind of placebo) which assumes that all OHb stretching wavenumbers are the same, independent of the type of solvate molecule or number of solvent units. This RMSD threshold can be straightforwardly adapted to computational submissions which only cover one of the $\approx 4 \times 10^3$ allowed distinct subsets of 3-11 wavenumbers.

Independent of the performance achieved by the participating computational models in HyDRA II and in the spirit of its mythological namesake,[26] we anticipate two important directions on the experimental side, given the relative scarcity of experimental references for uncharged systems in this field.[12] While most of the current HyDRA II database rests on spectra obtained in our Göttingen laboratory (see SI, chapter 3), the community could now make an effort to contribute carefully curated results from other laboratories. This will also help to flag potentially erroneous assignments.[27,28] To our knowledge, such databases already exist for isolated molecules[29] and to some extent also for a few hydrates.[30] Notifications to the corresponding author are welcome and a submission form will be provided. Furthermore, efforts to extend beyond the localised high frequency OHb oscillator towards more global spectroscopic probes such as the hydrogen bond librations[31] in isolated complexes should be encouraged despite their associated experimental challenges. Perhaps, (semi-)quantum matrix isolation work is sufficiently close to the gas phase[32] to help in filling this gap. These librations also play a key role in understanding local resonances in the OHb stretching range, as we confirm in the present work. Therefore, quantitatively predicting the combined OH stretch/libration dynamics in microhydration is a rewarding goal.

Author contributions

M.B.: data curation, formal analysis, investigation, methodology, project administration, validation, visualisation, writing – original draft, writing – review & editing; E.L.: investigation, writing – review & editing; F.K.: investigation, writing – review & editing; N.O.E.: investigation, writing – review & editing; E.S.: investigation, writing – review & editing; M.N.: investigation, writing – review & editing; N.O.B.L.: investigation, writing – review & editing; M.A.S.: conceptualisation, formal analysis, funding acquisition, investigation, methodology, resources, supervision, validation, writing – original draft, writing – review & editing. All authors have read and agreed to the published version of the manuscript.

Conflicts of interest

There are no conflicts of interest to declare. This article was completed without any knowledge of the content of computational submissions in the framework of the HyDRA II blind challenge. No experimental results on the HyDRA II test systems in this article including its draft versions were disclosed to computational participants of the HyDRA II blind challenge before the computational submission deadline. We are not aware of published or unpublished gas phase experimental OH stretching data from other research groups on the test

systems which might have given individual computational participants an advantage over others.

Data availability

Many data and all additional arguments supporting this article have been included as part of the supplementary information (SI). Supplementary information is available. See DOI: https://doi.org/10.1039/d6cp01096b.

The raw experimental spectra as well as ORCA output files are made available in GRO.data at https://doi.org/10.25625/G27IJZ. The results will be included into the HyDRA database at https://qmbench.net.

Acknowledgements

We thank Ricardo Mata for the organisation of this blind challenge and the faculty workshops for their instrument building and maintenance. We thank the numerous, for us still mostly anonymous computational participants for making HyDRA II work. We also thank Norbert Best from Bruker for decades of troubleshooting on our Fourier transform infrared spectrometers, without which the Es for our BEsT guesses would be missing in several instances. This work was funded by the Deutsche Forschungsgemeinschaft (DFG, German Research Foundation) – project number 389479699/GRK2455 and project number 405832858 (compute cluster). The carboxylic acid and hydroxylamine entries in the database and test set have profited from work carried out in the DFG-funded project 465181753. M. B. received financial support from the German Academic Scholarship Foundation (Studienstiftung des deutschen Volkes).

References

1 D. W. Hogg, *et al.*, A Blind Test of Photometric Redshift Prediction, *Astron. J.*, 1998, **115**, 1418–1422.
2 J. P. M. Lommerse, W. D. S. Motherwell, H. L. Ammon, J. D. Dunitz, A. Gavezzotti, D. W. M. Hofmann, F. J. J. Leusen, W. T. M. Mooij, S. L. Price, B. Schweizer, M. U. Schmidt, B. P. van Eijck, P. Verwer and D. E. Williams, A test of crystal structure prediction of small organic molecules, *Acta Crystallogr., Sect. B:Struct. Sci.*, 2000, **56**, 697–714.
3 H. C. Gottschalk, *et al.*, The first microsolvation step for furans: New experiments and benchmarking strategies, *J. Chem. Phys.*, 2020, **152**, 164303.
4 T. L. Fischer, M. Bödecker, A. Zehnacker-Rentien, R. A. Mata and M. A. Suhm, Setting up the HyDRA blind challenge for the microhydration of organic molecules, *Phys. Chem. Chem. Phys.*, 2022, **24**, 11442–11454.
5 W. Heisenberg, Über quantentheoretische Umdeutung kinematischer und mechanischer Beziehungen, *Z. Phys.*, 1925, **33**, 879–893.
6 J. R. Reimers, L. K. McKemmish, R. H. McKenzie and N. S. Hush, Non-adiabatic effects in thermochemistry, spectroscopy and kinetics: the general importance of all three Born–Oppenheimer breakdown corrections, *Phys. Chem. Chem. Phys.*, 2015, **17**, 24641–24665.
7 D. R. Lonsdale and L. Goerigk, The one-electron self-interaction error in 74 density functional approximations: a case study on hydrogenic mono- and dinuclear systems, *Phys. Chem. Chem. Phys.*, 2020, **22**, 15805–15830.
8 A. D. Boese, W. Klopper and J. M. L. Martin, Anharmonic force fields and thermodynamic functions using density functional theory, *Mol. Phys.*, 2005, **103**, 863–876.
9 R. A. X. Persson, V. Pattni, A. Singh, S. M. Kast and M. Heyden, Signatures of Solvation Thermodynamics in Spectra of Intermolecular Vibrations, *J. Chem. Theory Comput.*, 2017, **13**, 4467–4481.
10 R. Bombach, E. Honegger and S. Leutwyler, Solute-solvent interactions in microhydrate clusters: Carbazole-$(H_2O)_n$, *Chem. Phys. Lett.*, 1985, **118**, 449–454.
11 A. Potapov and P. Asselin, High-resolution jet spectroscopy of weakly bound binary complexes involving water, *Int. Rev. Phys. Chem.*, 2014, **33**, 275–300.
12 I. Neefjes, Y. Knattrup, H. Wu, G. B. Trolle, J. Elm and J. Kubečka, Thermodynamic benchmarking of hydrated atmospheric clusters in early particle formation, *Aerosol Res.*, 2026, **4**, 1–22.
13 T. L. Fischer, *et al.*, The first HyDRA challenge for computational vibrational spectroscopy, *Phys. Chem. Chem. Phys.*, 2023, **25**, 22089–22102.
14 QMbench – challenges for numerical quantum chemistry, https://qmbench.net/. 2021.
15 M. Suhm and F. Kollipost, Femtisecond single-mole infrared spectroscopy of molecular clusters, *Phys. Chem. Chem. Phys.*, 2013, **15**, 10702–10721.
16 H. C. Gottschalk, T. L. Fischer, V. Meyer, R. Hildebrandt, U. Schmitt and M. A. Suhm, A sustainable slit jet FTIR spectrometer for hydrate complexes and beyond, *Instruments*, 2021, **5**, 12.
17 N. O. B. Lüttschwager, The strength of the OH-bend/OH-stretch Fermi resonance in small water clusters, *Phys. Chem. Chem. Phys.*, 2024, **26**, 10120–10135.
18 T. L. Fischer, T. Wagner, H. C. Gottschalk, A. Nejad and M. A. Suhm, A rather universal vibrational resonance in 1:1 hydrates of carbonyl compounds, *J. Phys. Chem. Lett.*, 2021, **12**, 138–144.
19 E. Lwin, N. O. B. Lüttschwager and M. A. Suhm, The universal vibrational dynamics of water bound to tertiary amines: more than just Fermi resonance, *Phys. Chem. Chem. Phys.*, 2025, **27**, 5808–5820.
20 P. R. Franke, J. F. Stanton and G. E. Douberly, How to VPT2: Accurate and Intuitive Simulations of CH Stretching Infrared Spectra Using VPT2 + K with Large Effective Hamiltonian Resonance Treatments, *J. Phys. Chem. A*, 2021, **125**, 1301–1324.
21 E. Lwin, M. J. Gölz, N. O. B. Lüttschwager, M. A. Suhm, S. Käser, V. Andreichev, M. A. Brandes and M. Meuwly, Rotational, vibrational, conformational and diastereomeric dimer cooling of aminoalcohols in soft supersonic

expansions and the monohydrate of dimethylaminoethanol, *Phys. Chem. Chem. Phys.*, 2025, **27**, 17692–17703.
22 E. M. Brás, T. L. Fischer and M. A. Suhm, The hydrates of TEMPO: Water vibrations reveal radical microsolvation, *Angew. Chem., Int. Ed.*, 2021, **60**, 19013–19017.
23 W. Caminati, L. B. Favero, P. G. Favero, A. Maris and S. Melandri, Intermolecular hydrogen bonding between water and pyrazine, *Angew. Chem., Int. Ed.*, 1998, **37**, 792–795.
24 S. Melandri, M. E. Sanz, W. Caminati, P. G. Favero and Z. Kisiel, The Hydrogen Bond between Water and Aromatic Bases of Biological Interest: An Experimental and Theoretical Study of the 1:1 Complex of Pyrimidine with Water, *JACS*, 1998, **120**, 11504–11509.
25 N. O. Evers, S. M. Schweer and M. A. Suhm, Vibrational signatures of carboxylic acid microhydration for the HyDRA project, *Phys. Chem. Chem. Phys.*, 2025, **27**, 16507–16517.
26 S. Deacy, The Lernaean Hydra, *The Oxford Handbook of Monsters in Classical Myth*, 2024, 138.
27 G. Li, H. Xie and L. Jiang, Size-Specific Infrared Spectroscopy of Neutral Hydrated Clusters Based on a Vacuum Ultraviolet Free Electron Laser, *J. Phys. Chem. Lett.*, 2024, **15**, 4806–4814.
28 T. L. Fischer, C. V. Jensen, E. Lwin, D. Pal, H. G. Kjaergaard and M. A. Suhm, OH-stretching dynamics in trimethylamine monohydrate: what can we learn from three different direct absorption spectra?, *Phys. Chem. Chem. Phys.*, 2025, **27**, 11487–11491.
29 J. C. Zapata Trujillo and L. K. McKemmish, VIBFREQ1295: A New Database for Vibrational Frequency Calculations, *J. Phys. Chem. A*, 2022, **126**, 4100–4122.
30 R. Rahimi, N. Saban and I. Bar, Analyzing Spectral Similarities for Structural Identification Using a New Benchmark Database, *J. Phys. Chem. A*, 2026, **130**, 602–613.
31 D. Mihrin, J. Andersen, P. W. Jakobsen and R. Wugt Larsen, Highly localized H_2O librational motion as a far-infrared spectroscopic probe for microsolvation of organic molecules, *Phys. Chem. Chem. Phys.*, 2019, **21**, 1717–1723.
32 M. Bödecker, D. Mihrin, M. A. Suhm and R. Wugt Larsen, Regularities and Anomalies in Neon Matrix Shifts of Hydrogen-Bonded O–H Stretching Fundamentals, *J. Phys. Chem. A*, 2024, **128**, 7124–7136.